6th International Conference on Advances in Experimental Structural Engineering
11th International Workshop on Advanced Smart Materials and Smart Structures Technology
August 1-2, 2015, University of Illinois, Urbana-Champaign, United States

Wearable Carbon Nanotube Fabric Sensors for Strain and Temperature Monitoring

Long Wang[1], Kenneth J. Loh[2,*], Helen S. Koo[3]

1 Ph.D. Student, Dept. of Civil & Environmental Engineering, University of California, Davis, CA, United States. E-mail: lowang@ucdavis.edu.
*2 Associate Professor, Dept. of Civil & Environmental Engineering, University of California, Davis, CA, United States. E-mail: kjloh@ucdavis.edu. *Corresponding author*
3 Assistant Professor, Dept. of Design, University of California, Davis, CA, United States. E-mail: hskoo@ucdavis.edu.

ABSTRACT
The safe, efficient, and reliable operations of structural systems often rest upon the performance of the human operator. In numerous historical examples, catastrophic failure was a result of human-related factors. Thus, the objective of this research is to develop wearable fabric sensors for monitoring human performance. In particular, the goal is to monitor human physiological parameters, namely respiratory rate and body temperature, as a means for assessing human operator performance (*e.g.*, correlating them to fatigue or pre-existing medical conditions). This study presents preliminary results as to how these sensors can be fabricated, and their performance is characterized in the lab. First, multi-walled carbon nanotube (MWNT)-latex thin films with different MWNT concentrations were fabricated. The flexible films and stretchable fabric were combined to form a sandwich structure so that they could be worn directly. Second, its sensing properties were characterized by subjecting the fabric sensor to applied load patterns and temperature changes while its electrical response was measured. The results showed that the wearable fabric sensors' electrical response exhibited sensitivity to strain and temperature. Its flexibility and conformable nature make them ideally suited as wearable sensors.

KEYWORDS: *Carbon nanotube, human monitoring, strain, temperature, wearable fabric sensor*

1. INTRODUCTION

The safe, efficient, and reliable operations of land, air, and marine vessels or structures often depend on the performance of the human operator. Human error or fatigue has proven to be the cause of many historical catastrophes. For example, pilot fatigue was cited as one of the main reasons as to why Continental Airlines Flight 3407 (flying from Newark, NJ to Buffalo, NY on February 12, 2009) was unable to maintain sufficient airspeed and crashed mid-flight [1]. Similarly, on the ground, the lack of sleep and fatigue of air traffic controllers were responsible for numerous aviation disaster near misses [2]. On the other hand, the National Highway Traffic Safety Administration estimated that ~50,000 vehicular crashes (between July 3, 2005 and December 31, 2007) were due to, or at least partly, medical conditions such as seizures, black outs, diabetic reactions, and heart attacks [3]. Therefore, it can be argued that early detection and intervention (*e.g.*, allowing the first officer to take over for the pilot or having a driver pull over to the side of the road), and in general monitoring the performance of the human operator, could have prevented some of these fatal accidents.

One approach is to measure human vital signals (*e.g.*, respiratory rate and body temperature) using a wearable sensing system as a way of correlating and monitoring human physiological performance (*e.g.*, fatigue or pre-existing medical conditions). Two main approaches have been employed for developing these wearable sensors. The first is to utilize wireless body area networks (WBAN) in which discrete sensors (*e.g.*, accelerometers, electrocardiograph (ECG), and pulse-oximeter, among others) are worn on the human body and connected to a power source and wireless transceiver [4-6]. While these sensors are capable of providing high-quality and reliable measurements, form factor, power consumption, user comfort, and the need to wear an additional device are issues inherent to their design. The other body of work involves creating fabric-like sensors or *smart shirts* in which sensors are integrated with the user's garment [5, 7-9]. This technology enables better integration, but new types of thin and flexible sensing transducers are often needed. Regardless, these wearable sensors should be nonintrusive, noninvasive, comfortable, conformable, lightweight, low cost, and simple to use.

Lightweight, nanostructured, thin film sensors have emerged as a viable alternative to replace the bulky sensors used for wearable sensors and human performance monitoring. For instance, strain measurements can be particularly useful for measuring human body motions, physical activity, and fatigue, among others. In fact,

many types of highly stretchable and sensitive strain and pressure sensors have been developed by employing new materials, such as metal nanofibers [10-12], metal oxide fibers [13], and carbon nanotubes (CNT) [13-16]. For example, stretchable sensors have been fabricated by embedding CNTs within polymer thin film matrices, such as poly(dimethyl siloxane) (PDMS). Despite these advances in thin film sensing technologies, many of these systems have not been designed specifically for wearable fabric sensors, and better integration can be achieved. For instance, stretchable fabric is a more suitable flexible substrate than PDMS, since PDMS is not commonly found in typical garments or shirts [7].

Therefore, the objective of this study was to develop a nonintrusive, multifunctional, stretchable, and low-cost CNT-based fabric sensor that could be incorporated into clothes and worn directly for human performance monitoring. In particular, the aim was for the wearable fabric sensor to be able to measure respiratory rate (*i.e.*, by measuring breathing induced chest movements) and body temperature variations. This paper begins with a description of how these CNT-based fabric sensors were fabricated. Then, the experimental details of the strain and temperature sensing tests are presented, as well as the corresponding preliminary sensor characterization results. A brief summary and discussion of future work are included at the end of this paper.

2. EXPERIMENTAL DETAILS

2.1 Materials

All raw materials were used as purchased. Multi-walled carbon nanotubes (MWNT) were acquired from SouthWest NanoTechnologies (outer diameter: 6 to 9 nm; length: 5 μm; and purity: >95%). Other solvents, chemicals, and laboratory supplies for sensor fabrication were from Sigma-Aldrich and Fisher Scientific, except the latex solution, which was obtained from Kynar Aquatec. The sensor electrodes were prepared using single-strand wires from Digi-Key and silver paste from Ted Pella. The stretchable fabric used in this study was 100% nylon knit fabric. The Heatnbond iron-on adhesive (width: 15.9 mm) was from Therm-o-web.

2.2 Wearable Fabric Sensor Fabrication

CNT-based wearable fabric sensors were fabricated using a three-step process. The first step entailed dispersing MWNTs in a latex-based ink solution that could be used for spray-fabrication, which was based on previous work by Mortensen *et al*. [17]. The MWNT-latex inks were prepared by mixing MWNTs in a 2 *wt.*% poly(sodium 4-styrenesulfonate) (PSS) aqueous solution; trace amounts of N-methyl-2-pyrrolindinone (NMP) were also added. It should be mentioned that different amounts of MWNTs were mixed in the solution so that films with 1, 2, and 3 *wt.*% MWNTs could be fabricated. Then, dispersion was achieved by subjecting the solution to 60 min of high-energy probe sonication (3 mm tip, 150 W, 22 kHz), after which appropriate amounts of latex solution and 18 MΩ deionized water were added.

Second, the sensing element consisted of homogeneous and piezoresistive thin film sensors fabricated by spraying MWNT-latex ink solutions using a Paasche airbrush in a fume hood. Films were created by manually spraying MWNT-latex ink onto 25×75 mm^2 glass microscope slides. After spraying, the films were air dried inside the fume hood for at least 3 h. To improve their electrical properties, all of the freestanding films were also annealed at 80 °C for 12 h, followed by 150 °C for 3 h, using an StableTemp Model 282A vacuum oven [17, 18]. Figure 2.1 shows a scanning electron microscope (SEM) image of an MWNT-latex film, and the SEM image confirms the dispersion of MWNTs and the percolated morphology of the nanocomposite.

Finally, freestanding MWNT-latex thin films were integrated with the wearable fabric to obtain the final device. The annealed thin films were cut to 13×76 mm^2, and two electrodes were established on opposite ends of the sensor by drying silver paste on top of single-strand wires and the film. The gauge length between the two electrodes was 45 mm. Then, the MWNT-latex film (with electrodes attached) was sandwiched between the stretchable fabric and an iron-on adhesive; this was accomplished by ironing the iron-able tape directly on top of the film. Upon doing so, the wearable fabric sensor was trimmed to 16×112 mm^2. Each specimen was then allowed to cool down to room temperature before other tests were conducted. One can observe from Figure 2.2 that the fabric sensors were highly flexible, which is one of the essential features for wearable fabric sensors.

2.3 Electromechanical Characterization

As mentioned in Section 1, an aim of this work was to utilize the wearable fabric sensors for measuring strains due to chest movements and for determining human respiratory rate. In this preliminary laboratory study, the

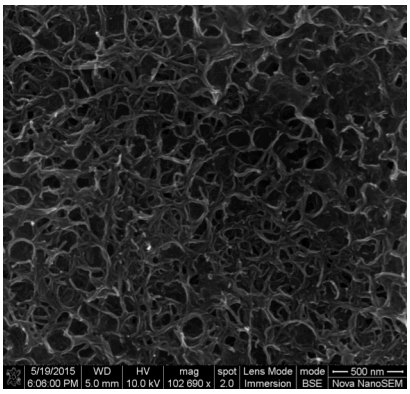

Figure 2.1 An SEM image of a 3 *wt.*% MWNT-latex thin film is shown.

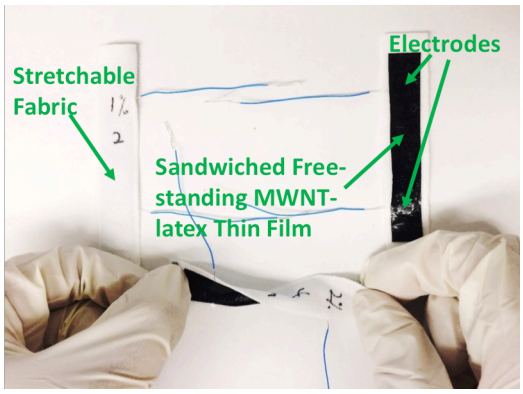

Figure 2.2 The MWNT-based wearable fabric sensors demonstrate excellent flexibility.

strain sensing properties of the fabric sensors were characterized by conducting electromechanical tests. Figure 2.3 shows the test setup, in which a fabric sensor was mounted in a Test Resources 150R load frame with both electrodes connected to an Agilent 34401A digital multimeter (DMM). Here, the DMM measured the electrical resistance of the wearable sensor as it was subjected to different load patterns. In addition, resistance, applied load, and crosshead displacement were recorded simultaneously using a customized *LabVIEW* program.

The test began with applying a static pretensioning force of 0.03 N so as to straighten the fabric sensor and to ensure that the specimen's longitudinal axis was parallel to the applied axial load. Although no visible slippage between the specimens and the serrated crosshead grips occurred, initial stress relaxation was common, which was very likely due to the fabric. After stress relaxation plateaued, which was indicated by stable unstrained resistance measurements, multiple 5-cycle tensile strain patterns up to 1% were applied to the specimens using a loading rate of 0.5 %-min^{-1}. In total, fabric sensors with 1, 2, and 3 *wt.*% MWNTs were tested and compared. Furthermore, due to CNTs' intrinsic light [19] and temperature sensitivity [19, 20], testing was conducted in the dark (by shielding specimens with a blackout curtain) and by keeping the ambient temperature constant.

2.4 Temperature Sensing Characterization

Besides measuring respiratory rate, it was also of interest to monitor human body temperature. Therefore, the temperature sensing properties of MWNT-latex fabric sensors were investigated by placing the sensors onto the surface of a Corning PC-620D hot plate (Figure 2.4). The actual temperature was measured using an Omega thermocouple adhered on top of the iron-on adhesive layer. Two Agilent DMMs were employed for simultaneously recording the thermocouple's direct current (DC) voltage response and the resistance of the MWNT-latex film. It should be mentioned that, during temperature sensing tests, the fabric sensors were unstrained and mounted flat on top of the hot plate's surface.

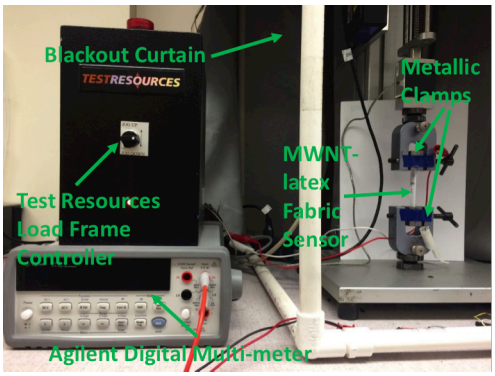

Figure 2.3 A fabric sensor was mounted in a Test Resources 150R load frame and connected to the digital multimeter.

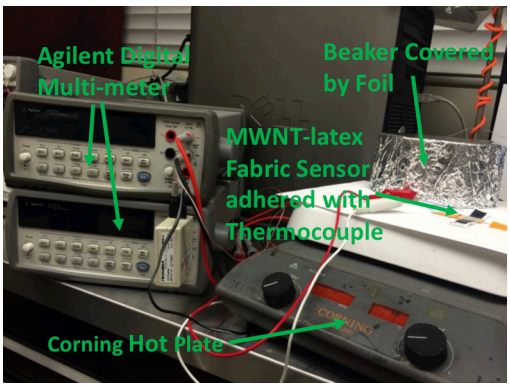

Figure 2.4 A thermocouple was adhered to a fabric sensor and placed on a hot plate for temperature sensing characterization tests.

Testing was performed by first increasing the temperature of the hot plate from room temperature (~25 °C) to ~65 °C, at which point, the hot plate was then switched off to allow the system to cool down naturally. The time span for the cooling down process, however, was different for the various cases investigated. In general, each sensor was subjected to three 65 °C heating and cooling cycles repeating every 50 min. The specimens were also shielded from light by covering the entire test setup with a large beaker covered with aluminum foil.

3. RESULTS AND DISCUSSIONS

3.1 Electromechanical Response

The strain sensing response of 1, 2, and 3 *wt.*% MWNT-latex fabric sensors were investigated by subjecting them to tensile cyclic load patterns (Section 2.3). The resistance time histories of representative films with different MWNT concentrations are overlaid with the applied strain patterns, as shown in Figures 3.1, 3.2, and 3.3. It can be observed that the resistance of the films increased in accordance with increasing strain, and this was consistent for sensors fabricated with different MWNT concentrations; the opposite was also true in that resistance decreased during unloading. These results confirmed thin film piezoresistivity.

In addition, Figure 3.4 shows the resistance response of a 3 *wt.*% MWNT specimen subjected to long-term testing, in which six sets of tensile cyclic loads were applied to the sensor. A few interesting features can be observed in Figure 3.4. First, there were significant and irreversible electric resistance changes that occurred immediately after applying the first tensile ramp. This was likely a result of permanent deformations in the fabric sensor (*i.e.*, potentially due to reconfigurations in the fabric gird pattern). Such irreversible resistance changes can be removed by applying cyclic loading to the wearable fabric sensors prior to their intended use. Second, the resistance time history response appears to be quite stable, but given enough time, resistance drifts still existed. This could be a result of the stretchable fabric's stress relaxation response.

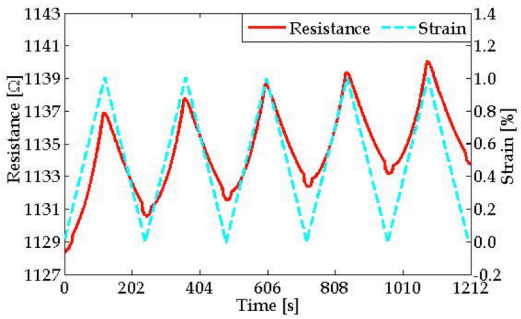

Figure 3.1 The change in resistance of a 1 *wt.*% MWNT-latex fabric sensor is overlaid with the applied 5-cycle strain pattern.

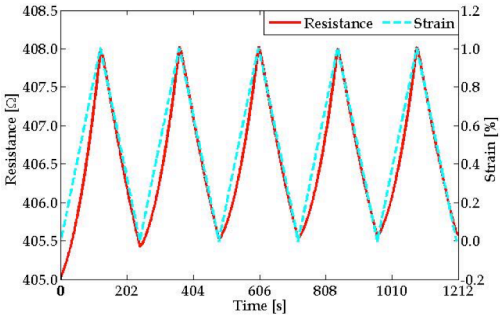

Figure 3.2 The change in resistance of a 2 *wt.*% MWNT-latex fabric sensor is overlaid with the applied 5-cycle strain pattern.

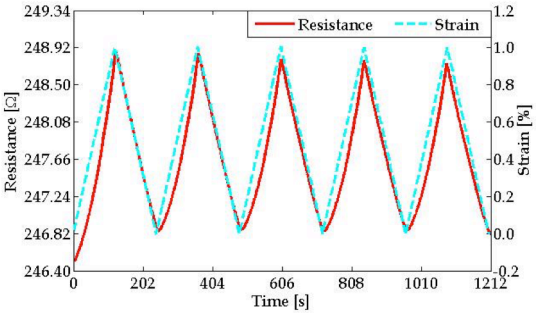

Figure 3.3 The change in resistance of a 3 *wt.*% MWNT-latex fabric sensor is overlaid with the applied 5-cycle strain pattern.

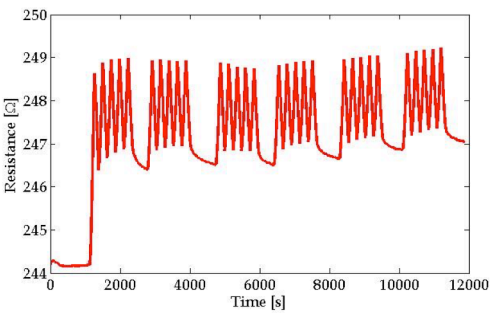

Figure 3.4 The long-term resistance time history of a 3 *wt.*% MWNT-latex fabric sensor subjected to multiple cyclic load patterns shows stable response.

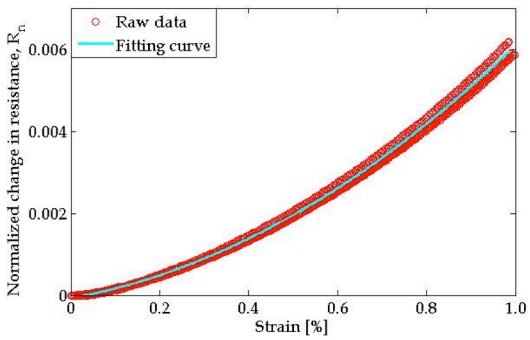

Figure 3.5 The normalized change in resistance of a 1 *wt.*% MWNT-latex fabric sensor is plotted as a function of applied strain (during four cycles), and the data was overlaid with a polynomial fit.

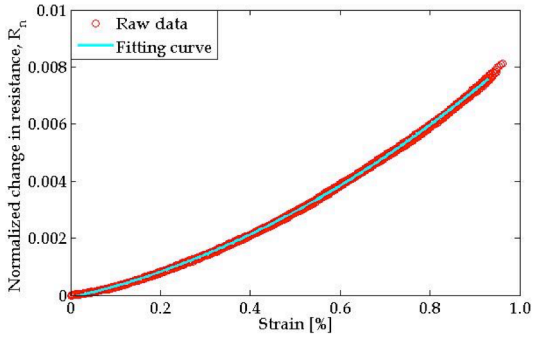

Figure 3.6 The normalized change in resistance of a 2 *wt.*% MWNT-latex fabric sensor is plotted as a function of applied strain (during four cycles) and the data overlaid with a polynomial fit.

Furthermore, as compared to the response of the 2 and 3 *wt.*% films, 1 *wt.*% MWNT-latex sensors exhibited irregular electrical resistance changes when applied strain was lower than 0.2%, as well as larger resistance drifts during the load tests. For these reasons, it was deemed that the 1 *wt.*% films were unsuitable for being used as wearable fabric sensors. Overall, the 2 and 3 *wt.*% fabric sensors exhibited the most reversible, repetitive, and stable electromechanical performance. Therefore, the remainder of the discussion in this section will be geared towards 2 and 3 *wt.*% MWNT-latex sensors.

The raw data was also processed by calculating normalized change in resistance (R_n) as follows:

$$R_n = \frac{R_i - R_0}{R_0} \tag{3.1}$$

where R_i indicates the electrical resistance of the film at any time instant, and R_0 is the stabilized unstrained resistance. As mentioned earlier, since resistance changes during the first load cycle were not fully reversible, R_0 was defined as the nominal resistance of the sensor at 0% strain, immediately before the start of the second load cycle. Figures 3.5 and 3.6 show the normalized resistance changes plotted with respect to applied strains and over four cycles of loading. In addition, a polynomial fit (Equation 3.2) was employed and fitted to the $R_n(\varepsilon)$ data, in which strain is ε, and A, B, and C are coefficients.

$$R_n(\varepsilon) = A\varepsilon^2 + B\varepsilon + C \tag{3.2}$$

It can be observed from Figures 3.5 and 3.6 that Equation 3.2 provided a suitable fit to the $R_n(\varepsilon)$ data. Also, no significant hysteresis was observed, and sensing response was highly repeatable over numerous loading cycles.

The sensitivity to strain of the 2 and 3 *wt.*% MWNT-latex fabric sensors was also investigated in this study. Strain sensitivity (S_S), or gage factor, can be defined as follows:

$$S_S = \frac{\Delta R_n}{\Delta \varepsilon} \tag{3.3}$$

where ΔR_n indicates the change in R_n when the applied strain changes by $\Delta\varepsilon$. Although normalized resistance change exhibits a polynomial relation with respect to strain, one could estimate S_S by fitting a linear line to the $R_n(\varepsilon)$ data. The slope of the linear least-squares best-fit line is equivalent to strain sensitivity (see Equation 3.3). However, in order to apply a reasonable linear best-fit to the data, an average strain cut-off was defined for each film, which is also shown in Table 3.1. $R_n(\varepsilon)$ data corresponding to strains smaller than the cut-off was not included for linear fitting. This study focused on the films' high-strain response, because their electromechanical response was more reliable and gave higher signal-to-noise ratios. In addition, wearable fabric sensors are expected to undergo large strains due to human body motions. The results of the linear fits are shown in Figures 3.7 and 3.8 and Table 3.1; based on the results obtained in this study, 3 *wt.*% films are characterized by higher strain sensitivities than the 2 *wt.*% sample set.

Table 3.1 Strain sensitivities of fabric sensors made with different MWNT concentrations

MWNT Concentrations	High Strain Region	Strain Sensitivity
2 *wt.*%	$\Delta\varepsilon \geq 0.39\%$	0.84 ± 0.05
3 *wt.*%	$\Delta\varepsilon \geq 0.33\%$	1.14 ± 0.04

3.2 Temperature Sensing Response

To characterize the temperature sensing performance of the MWNT-latex fabric sensors, the resistance (R) of the sensing films was monitored (and expressed as conductivity, σ), while temperature was altered (Section 2.4) and recorded using a thermocouple (Equation 3.4). Here, the MWNT-latex thin film's gauge length, width, and thickness are defined as l, w, and t respectively.

$$\sigma = \frac{l}{w \times t \times R} \tag{3.4}$$

Figures 3.9 and 3.10 show representative conductivity time histories of a 3 *wt.*% fabric sensor overlaid with the measured temperature (*i.e.*, by the thermocouple). It can be seen that that film's conductivity varied according to temperature variations, which was also observed by Vemuru *et al*. [20]; σ increased with increasing temperature. While the conductivity-temperature data matched closely during temperature ramp-up, there appeared to be a slight phase lag in the sensor's response during cooling (Figure 3.9). That is, it took longer time for the films to restore to their initial conductivity during cooling, as compared to what the thermocouple registered. Part of the reason could due to the thermocouple being located farthest away from the heat source and cooled slightly quicker, and a temperature gradient existed. In addition, Figure 3.10 shows the sensor's response to multiple thermal cycles, and the sensing response was found to be stable, repeatable, and with minimum phase lag (at least during heating). It should be noted that the phase lag observed during cooling was still present.

Figure 3.11 plots the normalized conductivity changes (σ_n) of three representative 1, 2, and 3 *wt.*% films (during heating) and with respect to the measured temperature. Here, σ_n was calculated by normalizing the change in conductivity of the film ($\Delta\sigma$) with respect to its baseline conductivity at room temperature (σ_0).

$$\sigma_n = \frac{\Delta\sigma}{\sigma_0} \tag{3.5}$$

The relationship between normalized conductivity change and change in temperature (ΔT) was found to be highly linear. Similar to the definition of strain sensitivity, temperature sensitivity (S_T) can be calculated using the change in normalized conductivity ($\Delta\sigma_n$) versus ΔT data.

$$S_T = \frac{\Delta\sigma_n}{\Delta T} \tag{3.6}$$

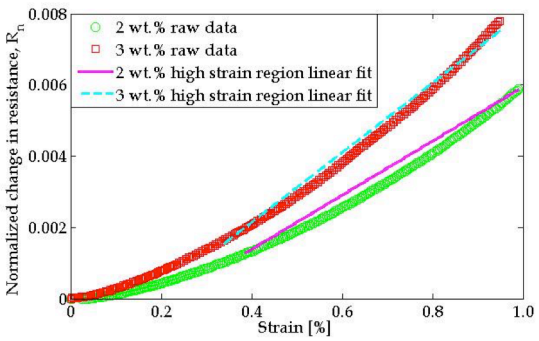

Figure 3.7 The normalized change in resistance of 2 and 3 *wt.*% MWNT-latex fabric sensors are plotted as a function of applied strain (one cycle), and the high strain regime was fitted to a linear best-fit line.

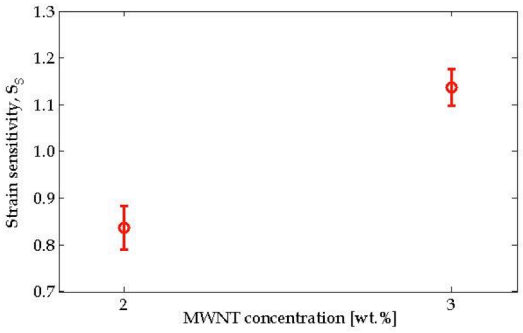

Figure 3.8 The average strain sensitivities (and standard deviation as error bars) of fabric sensors with different MWNT concentrations are shown.

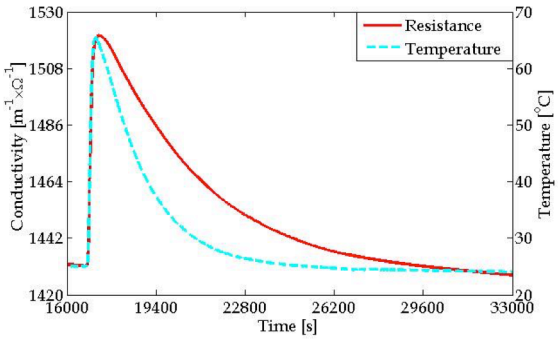

Figure 3.9 The sensor's conductivity time history is overlaid with the measured temperature.

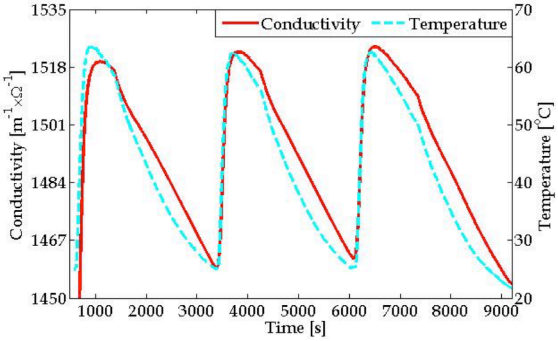

Figure 3.10 The conductivity and temperature time histories are overlaid to validate the MWNT-latex film's repeatable temperature sensing behavior.

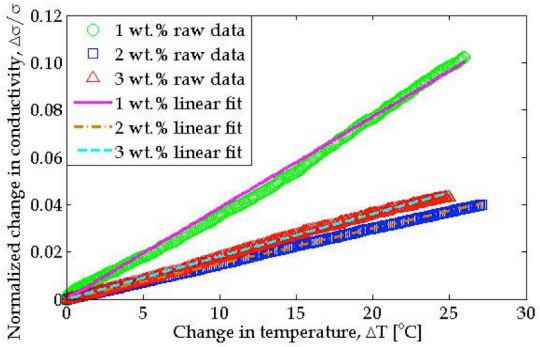

Figure 3.11 The normalized conductivity change of 1, 2, and 3 *wt.*% MWNT-latex fabric sensor are plotted as a function of temperature change to show their linear temperature sensing properties.

A linear least-squares regression line can be fitted to the data, and the slope of the fitted line is equivalent to S_T. Three representative sets of data (for 1, 2, and 3 *wt.*% MWNT-latex fabric sensors) are shown in Figure 3.11, along with the corresponding linear fits. Again, it is clear that the temperature sensing response is linear, but temperature sensitivity does not show clear trends with respect to MWNT concentrations. More tests and larger sample sizes need to be conducted in the future.

4. CONCLUSIONS

In this study, wearable MWNT-latex thin film sensors were fabricated (using airbrushing) and tested for human respiratory rate and body temperature monitoring applications. The sensing system was unique in that films with different MWNT concentrations were combined with stretchable fabric to form a sandwich structure, which can be worn directly and is nonintrusive for the user. First, by subjecting the sensors to cyclic tensile loads and analyzing the electrical resistance time histories, it was found that the resistance of 2 and 3 *wt.*% specimens exhibited stable and repetitive changes in tandem with applied strains. The films' electromechanical properties varied in a polynomial fashion with respect to applied strains. Second, the fabric sensors were also subjected to temperature sensing test. It was found that the conductivity of 1, 2, and 3 *wt.*% sensing films changed linearly in response to temperature variations. The film's conductivity increased as temperature was also increased. Future studies will focus on improving the structure of the fabric sensors so as to obtain more sensitive and stable sensing response. The next step will also involve validating this wearable technology using human subjects, as well as demonstrating that they can be used for monitoring respiratory rate and body temperature variations.

5. ACKNOWLEDGEMENTS

The authors thank the National Science Foundation (NSF) Faculty Early Career Development Program (CAREER) for the support of this research (under grant no. CMMI-1253564).

6. REFERENCES

1. Moore, K. (11 Oct. 2012) Pilot fatigue 'one of the biggest threats to air safety'. *BBC News*. URL: http://www.bbc.com/news/health-19837178
2. Ahlers, M. M. (10 Apr. 2007) NTSB: Air controller fatigue contributed to 4 mishaps. *CNN*. URL: http://www.cnn.com/2007/US/04/10/controller.fatigue/index.html?_s=pm:us
3. National Highway Traffic Safety Administration (2009). The contribution of medical conditions to passenger vehicle crashes. *U.S. Department of Transportation*. DOT HS 811 219.
4. Korhonen, I., Parkka, J., and van Gils, M. (2003). Health monitoring in the home of the future. *Engineering in Medicine and Biology Magazine, IEEE.* **22:3**, 66-73.
5. Pantelopoulos, A. and Bourbakis, N. G. (2010). A Survey on Wearable Sensor-Based Systems for Health Monitoring and Prognosis. *Systems, Man, and Cybernetics, Part C: Applications and Reviews, IEEE Transactions on.* **40:1**, 1-12.
6. Annavaram, M., Medvidovic, N., Mitra, U., Narayanan, S. S., Sukhatme, G., Meng, Z., Qiu, S., Kumar, R., Thatte, G., and Spruijt-Metz, D. (2008). Multimodal sensing for pediatric obesity applications. *Proceedings of the International Workshop on Urban, Community, and Social Applications of Networked Sensing Systems (UrbanSense)*. Raleigh, NC.
7. Castano, L. M. and Flatau, A. B. (2014). Smart fabric sensors and e-textile technologies: a review. *Smart Materials and Structures.* **23:5**, 53001-53028.
8. Lee, Y.-D. and Chung, W.-Y. (2009). Wireless sensor network based wearable smart shirt for ubiquitous health and activity monitoring. *Sensors and Actuators B: Chemical.* **140:2**, 390-395.
9. Paradiso, R., Loriga, G., and Taccini, N. (2005). A wearable health care system based on knitted integrated sensors. *Information Technology in Biomedicine, IEEE Transactions on.* **9:3**, 337-344.
10. Amjadi, M., Pichitpajongkit, A., Lee, S., Ryu, S., and Park, I. (2014). Highly stretchable and sensitive strain sensor based on silver nanowire–elastomer nanocomposite. *ACS nano.* **8:5**, 5154-5163.
11. Pang, C., Lee, G.-Y., Kim, T.-i., Kim, S. M., Kim, H. N., Ahn, S.-H., and Suh, K.-Y. (2012). A flexible and highly sensitive strain-gauge sensor using reversible interlocking of nanofibres. *Nature materials.* **11:9**, 795-801.
12. Gong, S., Schwalb, W., Wang, Y., Chen, Y., Tang, Y., Si, J., Shirinzadeh, B., and Cheng, W. (2014). A wearable and highly sensitive pressure sensor with ultrathin gold nanowires. *Nature communications.* **5**
13. Hu, B., Chen, W., and Zhou, J. (2013). High performance flexible sensor based on inorganic nanomaterials. *Sensors and Actuators B: Chemical.* **176**, 522-533.
14. Yamada, T., Hayamizu, Y., Yamamoto, Y., Yomogida, Y., Izadi-Najafabadi, A., Futaba, D. N., and Hata, K. (2011). A stretchable carbon nanotube strain sensor for human-motion detection. *Nature nanotechnology.* **6:5**, 296-301.
15. Song, X., Liu, S., Gan, Z., Lv, Q., Cao, H., and Yan, H. (2009). Controllable fabrication of carbon nanotube-polymer hybrid thin film for strain sensing. *Microelectronic Engineering.* **86:11**, 2330-2333.
16. Shin, M. K., Oh, J., Lima, M., Kozlov, M. E., Kim, S. J., and Baughman, R. H. (2010). Elastomeric conductive composites based on carbon nanotube forests. *Advanced materials.* **22:24**, 2663-2667.
17. Mortensen, L. P., Ryu, D. H., Zhao, Y. J., and Loh, K. J. (2013). Rapid Assembly of Multifunctional Thin Film Sensors for Wind Turbine Blade Monitoring. *Key Engineering Materials.* **569-570**, 515-522.
18. Kim, Y. A., Hayashi, T., Osawa, K., Dresselhaus, M. S., and Endo, M. (2003). Annealing effect on disordered multi-wall carbon nanotubes. *Chemical Physics Letters.* **380:3-4**, 319-324.
19. Loh, K. J., Kim, J., Lynch, J. P., Kam, N. W. S., and Kotov, N. A. (2007). Multifunctional layer-by-layer carbon nanotube–polyelectrolyte thin films for strain and corrosion sensing. *Smart Materials and Structures.* **16:2**, 429-438.
20. Vemuru, S. M., Wahi, R., Nagarajaiah, S., and Ajayan, P. M. (2009). Strain sensing using a multiwalled carbon nanotube film. *The Journal of Strain Analysis for Engineering Design.* **44:7**, 555-562.